UJEAS

UNIZIK JOURNAL OF ENGINEERING AND APPLIED SCIENCES

UNIZIK Journal of Engineering and Applied Sciences 5(1), June (2025), 2334 -2344
Journal homepage: https://journals.unizik.edu.ng/index.php/ujeas
PRINT ISSN: 2992-4383 || ONLINE ISSN: 2992-4391

Field Oriented Control for Efficient and Simplified Wind Power Generation Using DFIG

Abubakar I. A.[*1]., Mutari H. A.[2]
[1]Electrical/Electronic Technology Education Department FCE (Technical) Bichi, Kano State, Nigeria
[2]Department of Physics Bayero University, Kano State, Nigeria
[*]Corresponding Author's E-mail: dabo1429@gmail.com

Abstract
This paper presents the modeling, simulation, and performance analysis of a Doubly-Fed Induction Generator (DFIG)-based wind energy conversion system (WECS) using Field-Oriented Control (FOC) due to its structural simplicity and ability to meet desired dynamic performance requirements. The study includes comprehensive dynamic modeling of key WECS components from the wind turbine to the grid interface developed in a MATLAB/Simulink environment. The FOC strategy is applied to independently regulate active and reactive power, ensuring effective energy conversion and stable grid integration. Simulation results demonstrate the system's capacity to maintain steady active and reactive power output and achieve a low Total Harmonic Distortion (THD) of 4.57% in the grid voltage, indicating improved power quality. The novelty of this work lies in its system-wide modeling and performance validation of an FOC-controlled DFIG system in a compact, simulation-based approach suited for low-cost, efficient wind power applications. The results show that a well-implemented standard FOC approach can achieve effective control without the need for algorithmic complexity.

Keywords: AC/DC/AC converters, DFIG, Field Oriented Control, Grid, Renewable Energy, Wind Power Generation.

1. Introduction

The increasing urgency of addressing climate change and reducing greenhouse gas emissions has driven global efforts to transition to more sustainable energy systems. Among the various clean energy sources, wind power stands out due to its potential for reducing CO2 emissions and contributing to the global energy mix. As wind energy technologies advance, countries worldwide are increasingly turning to wind turbines to generate clean electricity. The Doubly Fed Induction Generator (DFIG) has gained prominence in wind farms due to its ability to operate at varying speeds, manage both real and reactive power, and maintain steady voltage and frequency despite rotor speed fluctuations (Sayeh et al., 2024). This ability makes DFIGs ideal for variable-speed wind energy systems, and much research has been conducted on their performance and optimization.

Despite these advantages, the DFIG system presents challenges in dynamic performance under fluctuating wind conditions, particularly in the effective control of both active and reactive power. To address these issues, various control strategies have been proposed. For instance, Backstepping with Lyapunov functions has been studied as a method for controlling electromagnetic torque and reactive power in DFIGs (Mensou et al., 2020). While effective in theory, this approach involves high computational effort, limiting its practicality in real-time applications. Fuzzy logic controllers (FLC) have also been explored as a way to enhance DFIG performance (Dida et al., 2020), offering flexibility in dealing with nonlinearities. However, the complexity and tuning difficulties of FLCs have made them less viable for cost-sensitive systems. Similarly, Artificial Neural Networks (ANN), used in direct torque control methods (Mahfoud et al., 2022), provide good performance but at the cost of high computational power and modeling challenges.

These existing methods, while valuable, often suffer from issues related to complexity, high computational cost, and inaccurate modeling, which limit their effectiveness in dynamic and real-world wind power generation systems. This paper proposes the use of Field-Oriented Control (FOC), a method known for its simplicity and efficiency. FOC enables effective management of both active and reactive power in DFIG systems with significantly lower computational requirements and greater ease of implementation compared to more complex methods. By focusing on the inherent advantages of FOC, we aim to provide a more robust, cost-effective, and practical solution to the challenges posed by current control methods.

2.0 DFIG Background Theory

DFIG systems function following the concept of electromagnetic induction, which involves the interaction of Lorentz's force and Faraday's law in contemporary renewable energy applications. By connecting the stator of the machine to the electrical grid, a magnetic field is produced by the stator windings, which is then synchronized with the predominant 50Hz frequency of the grid. Consequently, the stator's magnetic field oscillates at the same frequency as that of the grid (Abad et al., 2011). This connection is derived from Faraday's Law of Electromagnetic Induction expressed as:

$$\varepsilon = -\frac{d\phi_B}{dt} \tag{1}$$

Where,
dt = Change in time, $d\phi_B$= Change in Magnetic flux, ε = Induced emf, φ_B is the magnetic flux if the magnetic field varies sinusoidally as:

$B(t) = BoSin(2\pi ft)$ the induced EMF will vary sinusoidally with the same frequency at 50Hz. Lorentz's Force equation describes the interaction between the magnetic field and the moving charges within the generator. Thus,

$$F = q(V\ x\ B)$$
$$F = I\ x\ B \tag{2}$$

Where; F = Force on the conductor, B = Magnetic Flux density, V = Velocity of moving charges, q = electric charge, f = frequency, t = time and I = Current in the conductor

This force generates the torque that enables the DFIG to change the mechanical energy from the turbine to an electrical energy. While Faraday's law elucidates the induction of EMF, Lorentz's Force facilitates the physical interaction necessary for energy conversion (Abad et al., 2011). The AC/DC/AC converters connected to the rotor enable the machine to function effectively at varying wind speeds about the magnetic field of the stator. The EMF induced in the rotor arises from the relative movement between the magnetic field of the stator and that of the rotor. Generally, the controller of the rotor-side converter regulates electromagnetic torque and supplies a part of the reactive power required to maintain the machine's magnetization. On the other hand, the grid-side converter's controller is responsible for managing the DC link voltage (Abdelbaset et al., 2014). The frequency of the induced EMF is dictated by the slip frequency, which can be represented as:

$$F_{rotor} = F_{grid} - F_{rotor\ motion} \tag{3}$$

Where: $F_{rotor} = rotor\ frequency$, F_{grid} = Grid Frequency, $F_{rotor\ motion}$ = Frequency due to rotor motion determined by pole pairs and rotor speed

At synchronous speed, there is a lack of relative motion between the rotor and the stator's magnetic field, resulting in zero slip frequency. Consequently, Frotor = 0, and there is no induced EMF. When functioning at speeds below or above synchronous levels, there is a non-zero slip that enables the frequency of the induced EMF to correspond with the slip frequency, allowing power to be fed to the grid from both the stator and rotor windings. The rotor-side converter adjusts the rotor currents at both sub-synchronous and super-synchronous speeds to control active and reactive power by managing frequency and amplitude using field-oriented control. Meanwhile, the grid-side converter guarantees smooth power interaction with the grid at the stator frequency. The control strategies in DFIG oversee the

induced EMF to facilitate efficient power generation under varying wind speeds while ensuring synchronization with the grid.

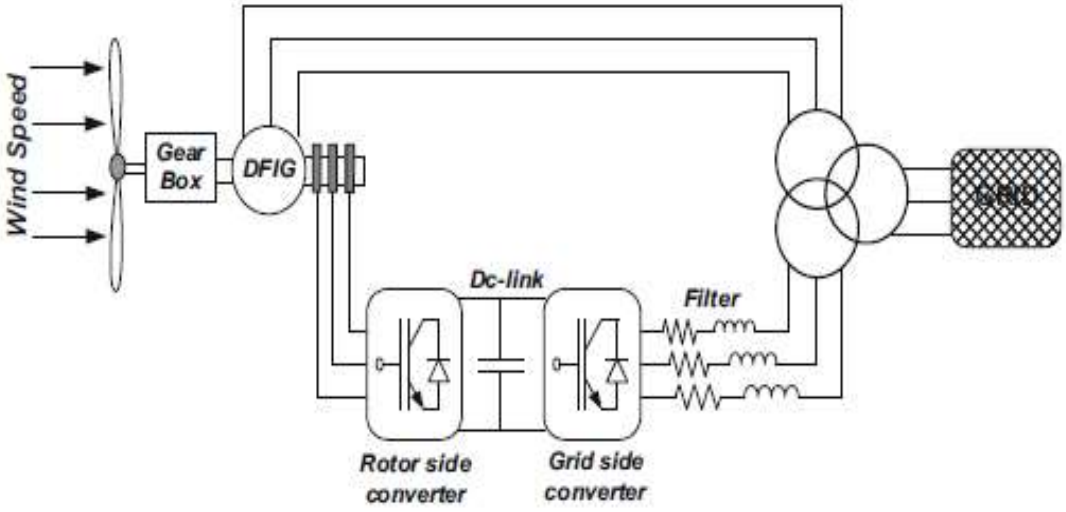

Figure 1: DFIG-based Wind Power generation (Abdelbaset et al., 2014)

3.0 Components Modeling

The components of the Wind Power Generation were examined, beginning with the conversion of kinetic energy from wind into mechanical energy and continuing until its connection with the electrical grid. By applying the laws of physics and neglecting mechanical and electrical losses, which are assumed to have no effect on the dynamic characteristics of the system, a dynamic model is created for all the components, as shown in Figure 1.

3.0.1 Wind Turbine modelling

A wind turbine is a mechanism that rotates to convert part of the wind's kinetic energy into mechanical energy at its rotor. The energy conversion process occurs in three steps. Initially, the wind's kinetic energy is changed into mechanical energy with the help of the wind turbine; in the next step, low shaft power is raised to high shaft power using a gearbox; and ultimately, this high shaft power is transformed into electrical energy. The aerodynamic wind power available over an area S, which is covered by the turbine blades, can be expressed by deriving the kinetic energy of the air mass that passes through this area.

$$P_w = \frac{1}{2}\rho S V^3 \quad (4)$$

Where ρ= the air density (≃1.22 kg/m3), $S = \pi R^2$: the region occupied by the turbine blades of radius R, and V represents the wind speed (m/s) and $P_w = wind\ power$

Based on the Betz limit (Telford, 1980), each wind turbine is capable of harnessing only a portion of the total power Pt; thus, every turbine is characterized by its power coefficient Cp (λ, β). This coefficient measures the turbine's aerodynamic efficiency, which is influenced by factors such as blade design, the pitch angle β, and the Tip speed ratio λ (Jabal Laafou et al., 2020). Consequently, the amount of aerodynamic power that is captured can be expressed as:

$$P_t = C_p(\lambda,\beta)P_w = \frac{1}{2}C_p(\lambda,\beta)\rho\pi R^2 V^3 \quad (5)$$

Where; β = Pitch angle, λ = Tip speed ratio, $P_t = turbine\ power$, $\rho = air\ density$

The mechanical torque appearing on the turbine rotor can therefore be subsequently represented by:

$$T_t = \frac{1}{2.\Omega} C_p(\lambda, \beta) \rho \pi R^2 V^3 \quad (6)$$

Where Ω_t is the turbine speed.

The power coefficient is generally represented as a nonlinear function of the Tip Speed Ratio λ and the Blade Pitch Angle β, with its theoretical maximum limit defined by Betz's law (Telford, 1980), (Bell, 1979). In this paper, CP (λ, β) is represented by the following function:

$$CP(\lambda, \beta) = 0.5176 \left(\frac{116}{\lambda} - 0.4\beta - 5\right) e^{-\frac{21}{\lambda}} + 0.0068\lambda \quad (7)$$

With;

$$\frac{1}{\lambda} = \frac{1}{\lambda + 0.08\beta} + \frac{0.035}{1+\beta^3} \quad (8)$$

$$\lambda = \frac{\Omega.R}{V} \quad (9)$$

Figure 2 illustrates how the power coefficient CP (λ, β) changes concerning λ for various values of β. It is evident that as the pitch angle β rises, the coefficient CP declines, leading to a decrease in the wind kinetic energy harnessed by the turbine.

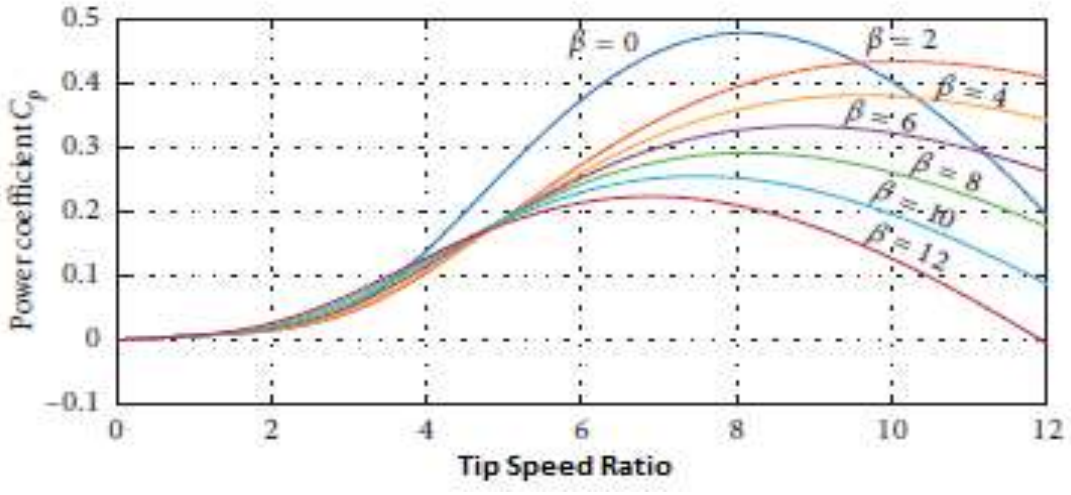

Figure 2: Evolution of the power coefficient C_P (λ, β)(Siraj et al., 2014)

3.0.2 DFIG Modelling

The DFIG comprises a 3-phase stator that is linked with the grid directly, along with a rotor that consists of 3-phase windings connected to the grid through slip rings fitted with sliding contacts and a double-stage power converter (Jabal Laafou et al., 2020). R. H. Park model is the most prevalent model for DFIG, providing the dynamic model in a d-q frame of reference that includes both transformations from three to two phases and two to three phases (Datta, 2015). Utilizing the DFIG electrical equivalent circuit depicted in Figure 3, the electrical equations for voltages, fluxes, and torque in the arbitrary d-q reference frames are expressed as:

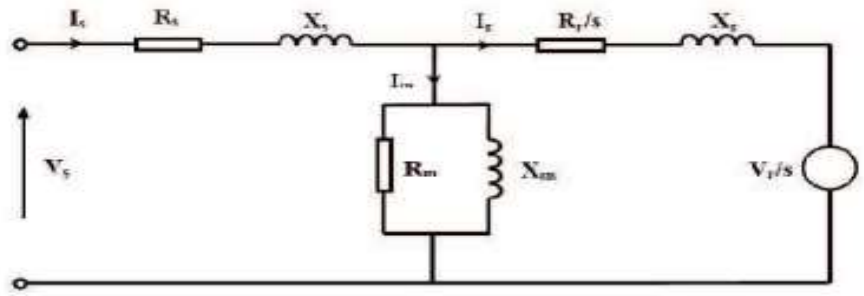

Figure 3: Electrical Equivalent Circuit of a DFIG (Siraj et al., 2014)

The stator and rotor voltages are expressed as:

$$V_{ds} = R_s I_{ds} + p\varphi_{ds} - \omega_s \varphi_{qs} \qquad \textit{Where} \quad p = \frac{d}{dt}$$

$$V_{qs} = R_s I_{qs} + p\varphi_{qs} + \omega_s \varphi_{ds} \tag{10}$$

$$V_{dr} = R_r I_{dr} + p\varphi_{dr} - (\omega_{s-} \omega_r)\varphi_{qr}$$

$$V_{qr} = R_r I_{qr} + p\varphi_{qr} + (\omega_{s-} \omega_r)\varphi_{dr}$$

The flux linkage equations of the stator and rotor can be related to the current and expressed as:

$$\varphi_{ds} = L_{ss} I_{ds} + L_m I_{dr}$$

$$\varphi_{qs} = L_{ss} I_{qs} + L_m I_{qr}$$

$$\varphi_{dr} = L_{rr} I_{dr} + L_m I_{ds} \tag{11}$$

$$\varphi_{qr} = L_{rr} I_{qr} + L_m I_{qs}$$

The electromagnetic torque generated by the DFIG is connected to the torque provided by the turbine and can be described as:

$$T_e = 1.5p(\varphi_{ds} I_{qs} - \varphi_{qs} I_{ds}) \tag{12}$$

4.0 The Vector Control Strategy

To improve the management of both active and reactive powers and enhance the efficiency of the DFIG system, a control strategy based on field-oriented control is employed, which involves transforming three-phase variables into synchronous frame variables within the d-q reference frames. Simulation of this control method incorporates the following assumptions given by (Siraj et al., 2014).

- The voltage across the stator resistance is regarded as insignificant.
- The q-axis leads d-axis by 90 degrees
- The vector of the stator flux is oriented with the d-axis of the stator.
- The grid voltage, amplitude and frequency are regarded as constant.
- The stator's magnetizing current is governed by the grid.

These assumptions result in the following.

$$V_{ds} = 0 \;\; \varphi_{ds} = \varphi_s \;\; V_{qs} = V_s \;\; \varphi_{qs} = 0 \tag{13}$$

Neglecting stator resistance

$$V_{ds} = 0 = p\varphi_{ds} - \omega_s\varphi_{qs}$$

$$V_{qs} = V_s = p\varphi_{qs} + \omega_s\varphi_{ds}$$

$$V_{dr} = R_r I_{dr} + p\varphi_{dr} - (\omega_{s-}\omega_r)\varphi_{qr} \tag{14}$$

$$V_{qr} = R_r I_{qr} + p\varphi_{qr} + (\omega_{s-}\omega_r)\varphi_{dr}$$

And the fluxes become

$$\varphi_{ds} = L_{ss} I_{ds} + L_m I_{dr}$$

$$0 = L_{ss} I_{qs} + L_m I_{qr}$$

$$\varphi_{dr} = L_{rr} I_{dr} + L_m I_{ds} \tag{15}$$

$$\varphi_{qr} = L_{rr} I_{qr} + L_m I_{qs}$$

Then,

$$V_{dr} = R_r I_{dr}\left(L_{rr} - \frac{L_m^2}{L_{ss}}\right) pI_{dr} - \left[(\omega_{s-}\omega_r)\left(L_{rr} - \frac{L_m^2}{L_{ss}}\right)\right] I_{qr} \tag{16}$$

$$V_{qr} = R_r I_{qr} + \left(L_{rr} - \frac{L_m^2}{L_{ss}}\right) pI_{qr} + (\omega_{s-}\omega_r)\left[\left(L_{rr} - \frac{L_m^2}{L_{ss}}\right) I_{dr} + \frac{L_m V_s}{\omega_s L_{ss}}\right.$$

The active and reactive powers generated in the stator, along with the rotor fluxes and voltages, can be expressed in terms of the rotor currents as:

$$P_s = -\frac{L_m V_s}{L_{ss}} * I_{qr} \tag{17}$$

$$Q_s = -\frac{V_s^2}{\omega_s L_{ss}} - \frac{L_m V_s}{L_{ss}} * I_{dr}$$

Consequently, the reference currents can be expressed concerning the active and reactive powers as follows:

$$I_{qr} = -\frac{L_{ss} P_s}{L_m V_s}$$

$$\mathrm{I}_{dr} = \left(Q_s - \frac{V_s^2}{\omega_s L_{ss}}\right) * -\frac{L_{ss}}{V_s L_m} \tag{18}$$

5.0 Simulation Set Up

Using all the equations and the control variables, the system was developed and simulated in a Matlab/Simulink as seen in figure 4.

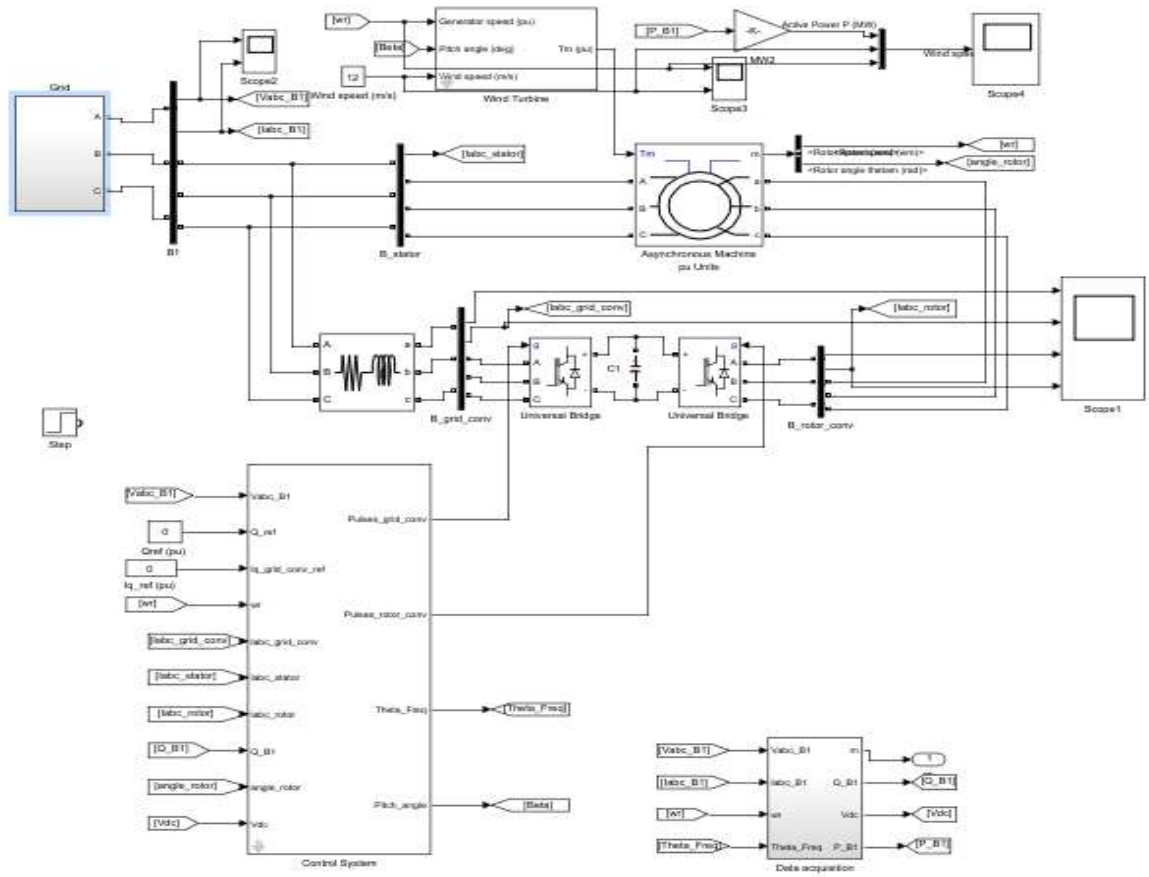

Figure 4: Simulation Set-up of a DFIG System

The parameters of the DFIG, Wind Turbine, and the control settings utilized for the simulation are provided in the tables below.

Table 1: DFIG Machine Parameters

Parameters	Values
Rated Power P	1.5Mw
Rated Voltage V	575V
Nominal Frequency F	60Hz
Poles Number P	3
Stator Res. R_s	0.00706mohm
Rotor Res. R_r	0.005mOhm
Leakage Inductance L_{ls}	0.171mH
Leakage Inductance L_{lr}	0.156mH
Magnetizing Inductance L_m	2.9mH

Table 2: Turbine Parameters

Parameters	Values
Rated Power	1.5MW
Rated Speed	12m/s
Air Density	1,225kg/m3
Mechanical power P_{mech}	0.73MW
Rotational Speed	1.2m/s

Table 3: Grid Parameters

Parameters	Values
Voltage at DC-link V_{dc}	1200v
Capacitor at DC-Link C	0.06microF
Filter Resistance R_f	0.03Ohms
Filter Inductance L_f	3mH

Table 4: Controller Parameters

	Parameters	Values
Turbine	Pitch Angle gain K_p	500
	Max Pitch Angle	45°
	Max. Change of Pitch angle	2°
Filter	Cut-off freq.	1000Hz
	Damping Factor	0.707
	Sample Time	5e-006s
Grid Voltage Gains	K_p and K_i	2.5, 500
Grid Current Gains	K_p and K_i	0.3, 8
DC-Link Voltage Gains	K_p and K_i	0.002, 0.05

3.0 Result and Discussion

The developed DFIG-based wind energy conversion system was simulated in MATLAB/Simulink using the derived dynamic models and the implemented Field-Oriented Control (FOC) strategy. The simulation setup incorporated real-world electrical and mechanical parameters for the DFIG, wind turbine, and control systems. The focus of the results was to assess system behavior under typical operating conditions and validate the effectiveness of FOC in regulating active and reactive power and improving power quality.

6.0.1 Active and Reactive Power Regulation

Figure 5 illustrates the system's active power response. After an initial transient phase, the active power output stabilized at the desired value within 0.2 seconds. This was achieved by regulating the q-axis component of the rotor current via the FOC controller. Such fast tracking and stabilization are comparable to results in [Siraj et al., 2014], which also employed FOC but with more complex tuning strategies. The system used in this study, however, maintains similar performance with reduced control complexity.

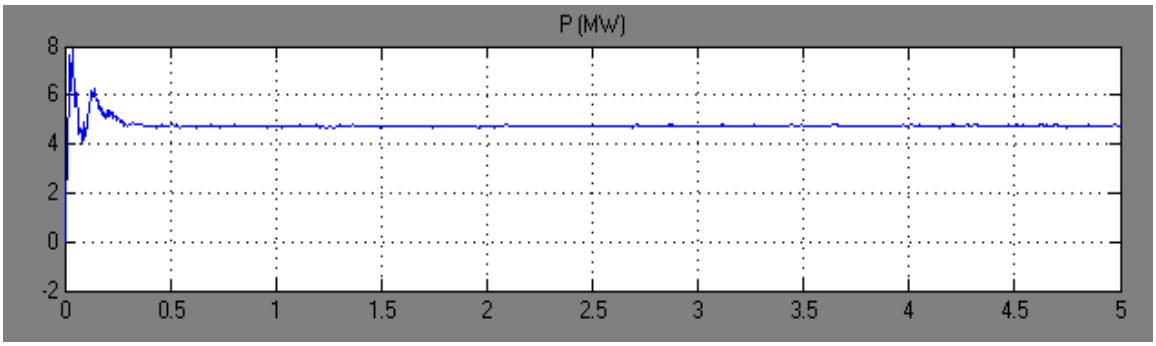

Figure 5: The Active Power P

Figure 6 shows the reactive power performance. It stabilized post 0.2 seconds, demonstrating effective decoupled control via the d-axis rotor current. This validates the FOC scheme's ability to independently regulate reactive power, which is vital for voltage support and grid stability. Unlike the approach in [Jabal Laafou et al., 2020], which incorporated adaptive pitch control, this study achieved stability using fixed controller gains, thereby highlighting the simplicity and effectiveness of the selected FOC scheme.

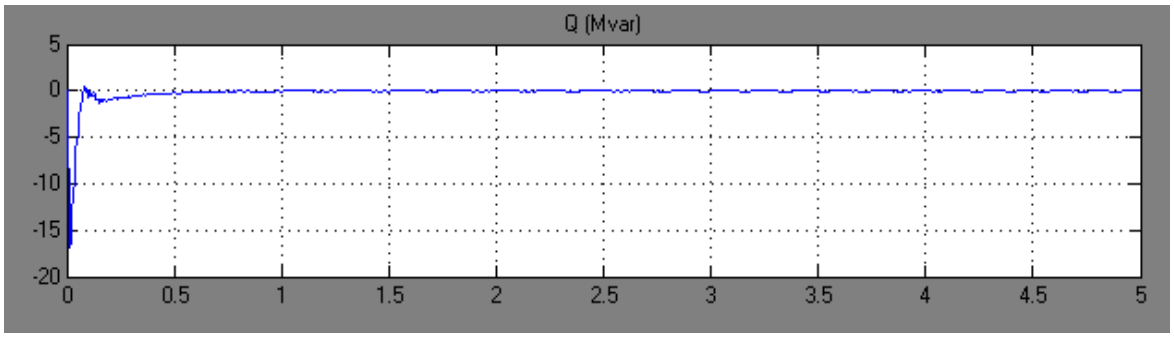

Figure 6: The Reactive Power Q

6.0.2 Grid side Voltage, Current, and Harmonic Performance

Figures 7(a) and (b) present the three-phase voltage and current waveforms at the grid side. The signals settled into steady-state sinusoidal profiles after a short transient of about 0.04 seconds. This confirms the robustness of the FOC system in facilitating smooth grid integration without distortion or oscillations.

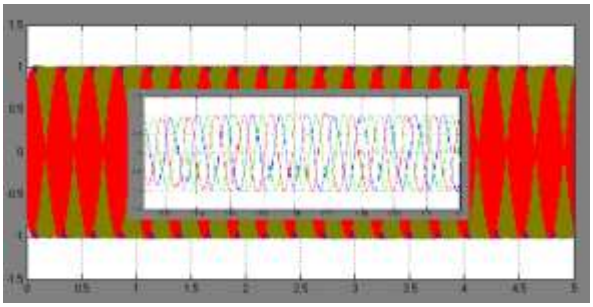

Figure 7(a) Grid Voltage

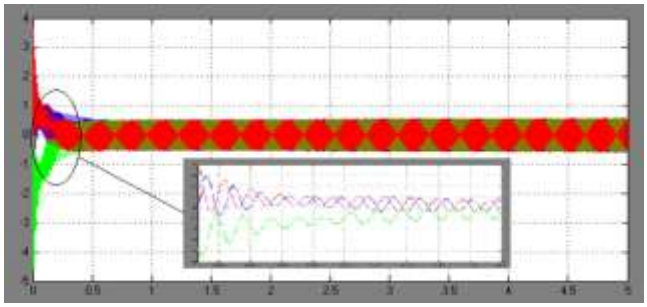

Figure 7(b) Grid Current

To assess power quality, harmonic analysis was conducted using the Fast Fourier Transform (FFT). Figure 7(c) shows that the Total Harmonic Distortion (THD) in the grid voltage was 4.57%, which is below the IEEE 519 recommended limit of 5%. This result not only supports the claim made in the abstract but also compares favorably with other FOC-based DFIG studies (e.g., Datta, 2015), where THD was reduced using additional harmonic filtering components. In contrast, our setup achieves acceptable THD through a well-tuned control strategy alone, underscoring the system's efficiency and cost-effectiveness.

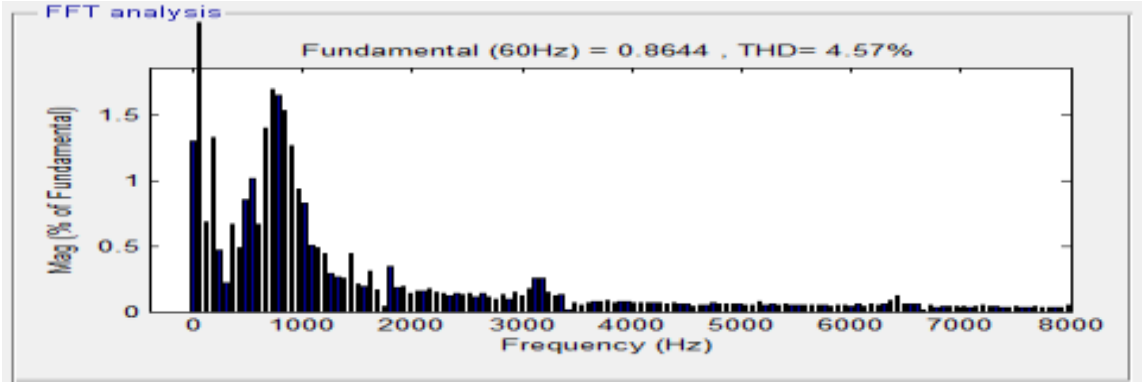

Figure 7(c) FFT Analysis

6.0.3 DC-Link Voltage Stability

Figure 8 presents the DC-link voltage response. The voltage reached and maintained the target value of 1200 V after 0.5 seconds, reflecting successful control via the grid-side converter. This performance metric is crucial in ensuring uninterrupted energy delivery and proper decoupling between the machine and the grid. The result is in alignment with findings from [Telford, 1980], where DC-link fluctuations were minimized using feedback-based control.

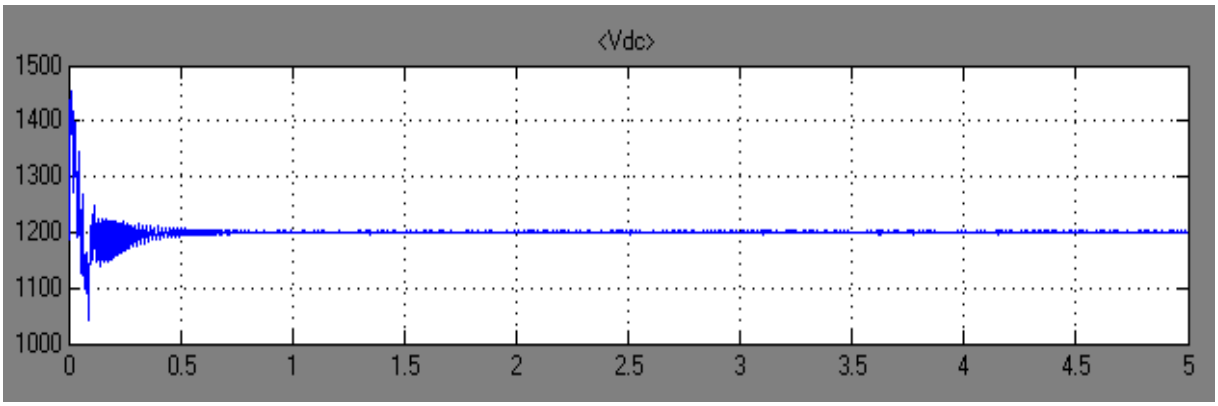

Figure 8: DC-Link Voltage

4.0. Conclusion

This This study focused on the modeling, simulation, and performance analysis of a Doubly-Fed Induction Generator (DFIG)-based wind energy conversion system using Field-Oriented Control (FOC). The main objective was to demonstrate that standard FOC without modifications can be used effectively in wind applications to manage active/reactive power and enhance power quality. Through detailed dynamic modeling of each system component and simulation in MATLAB/Simulink, the system was shown to track reference power values efficiently, maintain DC-link voltage stability, and limit harmonic distortion to 4.57%. These results affirm the suitability of FOC for decentralized and cost-sensitive wind energy applications. In comparison with existing literature, this work offers a unified simulation and analysis framework, proving that even without advanced algorithmic techniques, reliable and clean power delivery can be achieved. The findings contribute to the growing field of simplified wind energy conversion strategies, particularly for small and medium-scale renewable energy systems. Future work may focus on experimental validation using hardware-in-the-loop (HIL) systems, integration of fault ride-through capability, or comparative studies involving other control strategies such as Model Predictive Control or Artificial Intelligence-based tuning to assess performance trade-offs under varied wind profiles.

Recommendation

It is recommended that the future work may focus on experimental validation using hardware-in-the-loop (HIL) systems, integration of fault ride-through capability, or comparative studies involving other control strategies such as Model Predictive Control or Artificial Intelligence-based tuning to assess performance trade-offs under varied wind profiles.

References

Abad, G., López, J., Rodríguez, M. A., Marroyo, L., & Iwanski, G. 2011 Doubly Fed Induction Machine: Modeling and Control for Wind Energy Generation. In *Doubly Fed Induction Machine: Modeling and Control for Wind Energy Generation*. https://doi.org/10.1002/9781118104965

Abdelbaset, A., Mohamed, Y. S., El-Sayed, A.-H. M., & Abozeid, A. A. E. H. 2014. Wind turbine driven doubly-fed induction generator. In *RTDS Technol. Inc. Winnipeg, MB, Canada*. http://link.springer.com/10.1007/978-3-319-70108-0

Bansal, R. C. 2005. Three-phase self-excited induction generators: An overview. *IEEE Transactions on Energy Conversion*, *20*(2), 292–299. https://doi.org/10.1109/TEC.2004.842395

Bell, D. A. 1979. Fundamentals of Wind Energy. In *Physics Bulletin* (Vol. 30, Issue 12). https://doi.org/10.1088/0031-9112/30/12/057

Cherifi, D., & Miloud, Y. 2020. Hybrid control using adaptive fuzzy sliding mode control of doubly fed induction generator for wind energy conversion system. *Periodica Polytechnica Electrical Engineering and Computer Science*, *64*(4), 374–381. https://doi.org/10.3311/PPee.15508

Datta, S. 2015. *Performance Analysis of a DFIG based Variable Speed Wind Energy Conversion System*. *January*.

Dida, A., Merahi, F., & Mekhilef, S. 2020. New grid synchronization and power control scheme of doubly-fed induction generator based wind turbine system using fuzzy logic control. *Computers and Electrical Engineering*, *84*. https://doi.org/10.1016/j.compeleceng.2020.106647

Jabal Laafou, A., Ait Madi, A., Addaim, A., & Intidam, A. 2020. Dynamic Modeling and Improved Control of a Grid-Connected DFIG Used in Wind Energy Conversion Systems. *Mathematical Problems in Engineering*, *2020*. https://doi.org/10.1155/2020/1651648

Mahfoud, S. A. I. D., Derouich, A. Z. I. Z., Ouanjli, N. EL, & Mahfoud, M. EL. 2022. Enhancement of the Direct Torque Control by using Artificial Neuron Network for a Doubly Fed Induction Motor. In *Intelligent Systems with Applications* (Vol. 13, Issue January). Elsevier Ltd. https://doi.org/10.1016/j.iswa.2022.200060

Mensou, S., Essadki, A., Nasser, T., Idrissi, B. B., & Ben Tarla, L. 2020. Dspace DS1104 implementation of a robust nonlinear controller applied for DFIG driven by wind turbine. *Renewable Energy*, *147*, 1759–1771. https://doi.org/10.1016/j.renene.2019.09.042

Naik, K. A., Gupta, C. P., & Fernandez, E. 2020. Design and implementation of interval type-2 fuzzy logic-PI based adaptive controller for DFIG based wind energy system. *International Journal of Electrical Power and Energy Systems*, *115*(August 2019). https://doi.org/10.1016/j.ijepes.2019.105468

Pena, R., & Clare, J. C. 2017. *supplying an isolated load from a variable speed wind turbine A doubly fed induction generator using converters s variable speed wind turbine*. *October 1996*. https://doi.org/10.1049/ip-epa

Rached, B., Elharoussi, M., & Abdelmounim, E. 2020. Design and investigations of MPPT strategies for a wind energy conversion system based on doubly fed induction generator. *International Journal of Electrical and Computer Engineering*, *10*(5), 4770–4781. https://doi.org/10.11591/ijece.v10i5.pp4770-4781